Journal of Achievements in Materials and Manufacturing Engineering
VOLUME 55
ISSUE 2
December
2012

Modification of non-metallic inclusions in high-strength steels containing increased Mn and Al contents

A. Grajcar [a,*], M. Kamińska [b], U. Galisz [c], L. Bulkowski [c], M. Opiela [a], P. Skrzypczyk [a]

[a] Institute of Engineering Materials and Biomaterials, Silesian University of Technology, ul. Konarskiego 18a, 44-100 Gliwice, Poland
[b] Institute of Non-Ferrous Metals, ul. Sowińskiego 5, 44-100 Gliwice, Poland
[c] Institute for Ferrous Metallurgy, ul. K. Miarki 12-14, 44-100 Gliwice, Poland
* Corresponding e-mail address: adam.grajcar@polsl.pl

Received 24.10.2012; published in revised form 01.12.2012

Materials

ABSTRACT

Purpose: The aim of the work is to determine an influence of the effectiveness of the modification of the chemical composition and morphology of non-metallic inclusions by rare earth elements in advanced high strength steels (AHSS) with increased Mn and Al contents.
Design/methodology/approach: The effects of the modification of non-metallic inclusions were assessed in four thermomechanically rolled AHSS containing various Mn (3 and 5%) and Nb (0 and ~ 0.04%) concentration. The surface fraction, surface area and aspect ratio were determined at longitudinal sections of the sheets with a thickness of 3.3 mm. The chemical composition of particles was investigated using point analysis and mapping by means of EDS and WDS techniques.
Findings: The refining treatment of a liquid steel has an important effect on the sulphur content in a steel, a surface fraction of non-metallic inclusions, their deformability during hot-rolling and morphology. On the other hand the addition of mischmetal does not affect an inclusion size. The chemical composition of particles is independent on the Mn content in a range investigated, i.e., from 3 to 5%. The steels with the addition of REE contain totally modified, fine oxysulfides of Ce, La and Nd whereas the steel not subjected to the refining treatment contains elongated MnS, complex MnS + AlN compounds and AlN particles decorated in the outside zone by MnS and Al_2O_3.
Practical implications: The knowledge of the stereological parameters of non-metallic inclusions and their morphology are of primary importance for the steelmaking and hot-working technologies of steel products.
Originality/value: An effectiveness of the modification of the chemical composition and morphology of non-metallic inclusions by REE in advanced high-strength steels with increased Mn and Al contents is addressed in the current study.
Keywords: Metallic alloys; High strength steels; Thermomechanical rolling; Non-metallic inclusions

Reference to this paper should be given in the following way:
A. Grajcar, M. Kamińska, U. Galisz, L. Bulkowski M. Opiela, P. Skrzypczyk, Modification of non-metallic inclusions in high-strength steels containing increased Mn and Al contents, Journal of Achievements in Materials and Manufacturing Engineering 55/2 (2012) 245-255.

1. Introduction

Advanced high-strength steels (AHSS) for the automotive industry contain various fractions of soft and hard phases allowing to obtain the beneficial balance between strength, ductility and technological formability of steel sheets. The microstructure of Dual Phase (DP) steel consists of ferrite and martensite [1,2] whereas the multiphase microstructure of TRIP (TRansformation Induced Plasticity) steel contains ferrite, bainite and retained austenite [3-9]. New demands of the automotive industry for relatively low-cost steel sheets characterized by tensile strength above 1000 MPa require further searching of new chemical composition solutions or modification of processing routes for conventional steels. Advanced ultra-high strength steels contain a higher fraction of hard phases, i.e., acicular ferrite, bainite or martensite [10-20] compared to AHSS containing polygonal ferrite as a matrix. A key microstructural constituent of advanced multiphase steels is retained austenite with the amount from 10 to 30%. This phase ensures the required ductility level, similarly to its effect in single-phase high-manganese austenitic alloys containing from 18 to 30 wt.% Mn [21-25]. However, the low-cost demands decide that the Mn content is limited up to about 12 wt.% in recently designed medium-Mn high-strength automotive steels [10-15,19,20,26]. The high amount of retained austenite can be obtained by chemical stabilization (Mn alloying) or mechanical stabilization related to grain size refinement by reverse $\alpha' \rightarrow \gamma$ phase transformation during continuous annealing (cold-rolled sheets) or using thermomechanical processing (hot-rolled sheets) [11, 13-15,19,20,26]. Final mechanical and technological properties of multiphase steel sheets are dependent both on the retained austenite fraction and its mechanical stability against strain-induced martensitic transformation during cold forming [4,6,11,16,17,26].

It is well known that the technological formability of steel sheets is highly dependent on the fraction, distribution and morphology of non-metallic inclusions. AHSS contain increased concentrations of Mn, Al and Si. Therefore, the metallurgical process, continuous casting and hot-working of AHSS should take into account the possibility of enhanced forming of sulfides, oxides and silicates affecting negatively formability of steel sheets. Unfortunately, there is not sufficient data covering this problem in the literature. Elongated sulfide inclusions or chain-like crushed oxide inclusions are a reason of the anisotropy of ductile properties as well as lowered bendability and stretch-flangeability of steel sheets [17,27]. Yu et al. [9] and Lacroix et al. [28] reported that the nucleation of microvoids and their coalescence leading to forming of microcracks take place at ferrite-martensite phase boundaries or at non-metallic inclusions. Results of Sugimoto et al. [17] confirmed that the reasons of cracks occurring on hole-expanding of steel sheets (high stretch stresses) are voids formed on previous hole-punching at matrix-second phase interface.

Some examples of non-metallic inclusions occurring in different grades of AHSS together with the thermodynamic calculations of their equilibrium composition and precipitation behaviour can be found in [29-31]. To reduce the deformability of non-metallic inclusions during hot-working, the modification of their chemical composition and morphology by calcium compounds or rare earth elements (REE) is carried out [32-35]. It is reported in [32] that the total modification of oxysulfide non-metallic inclusions in Nb-Ti-microalloyed steels containing 1.5% Mn and 0.004% S requires adding 2 g of mischmetal per 1 kg of steel. On the other hand, the similar addition of rare earth elements to the high-manganese steels containing about 25% Mn and 0.013-0.017% S enables only the partial modification of outside zones of non-metallic inclusions.

2. Experimental procedure

The paper presents a problem of the modification of chemical composition of non-metallic inclusions and their hot-working behaviour in four model high-strength steels containing a different Mn content and Nb microaddition. The steels contain 3 or 5% Mn, 1.5% Al and increased concentration of Mo (Table 1). Manganese content and Nb-microaddition are the basis for the designation of steels (3Mn, 3MnNb, 5Mn, 5MnNb). The steel ingots were produced by vacuum induction melting in the Balzers VSG-50 furnace (Institute for Ferrous Metallurgy, Gliwice, Poland). Basic charge consisted of Armco iron and alloy additions in the form of pure elements (C, Si, Mn, Mo, Al) and ferroalloys (Fe-Nb). Iron and molybdenum were loaded into the crucible while the alloying additions were distributed into individual compartments of the alloy hopper, in the sequence complying with their subsequent introduction into the bath (Al, Si, Mn, C, Fe-Nb). In order to modify non-metallic inclusions, rare earth elements as mischmetal (~50% Ce, ~20% La, ~20% Nd) were also added to three melts (3MnNb, 5Mn, 5MnNb). Mischmetal was added as the last addition in the amount of 2 g per 1 kg of steel.

Table 1.
Chemical composition of the investigated steels (mass content, %)

	Steel designation			
	3Mn	3MnNb	5Mn	5MnNb
C	0.17	0.17	0.16	0.17
Mn	3.3	3.1	4.7	5.0
Al	1.7	1.6	1.6	1.5
Si	0.22	0.22	0.20	0.21
Mo	0.23	0.22	0.20	0.20
Nb	-	0.04	-	0.03
P	0.010	0.008	0.008	0.008
S	0.014	0.005	0.004	0.005
N	0.0043	0.0046	0.0039	0.0054
O	0.0004	0.0006	0.0004	0.0004

Liquid metal was cast under argon atmosphere from the temperature of 1545°C into a hot-topped closed-bottom wide-end-up cast iron mould with internal dimensions: bottom - ∅ 122 mm, top - ∅ 145 mm, height - 200 mm (without ingot head). Forging of ingots was carried out using high-speed hydraulic press applying 300 MN of force to obtain 22x170 mm flat samples. The range of hot-working temperature was equal to 1200-900°C with inter-operational reheating in order to prevent the temperature drop of ingots below 900°C. Subsequently, flat samples were roughly hot-rolled in four passes (true strain: 0.19, 0.28, 0.29, 0.24) into 9 mm thick sheets. After finishing rolling at 900°C the sheets were air cooled to room temperature (RT).

The final thermomechanical rolling was carried out in five passes to a sheet thickness of about 3.3 mm. A semi-industrial two-high reversing mill with a roll diameter of 550 mm was used to simulate the thermomechanical processing paths (Institute for Ferrous Metallurgy, Gliwice). The 9×170×500 mm sheet samples were soaked in a furnace for 25 min. at the temperature of 1200°C. After 20 s the sheets were pushed through the rolling mill, where five deformation steps were applied. The interpass times between successive deformation steps were equal from 5 to 8 s. After the final deformation at about 800°C the specimens were cooled in the different way depending on the steel type. The 3Mn and 3MnNb steels were initially air-colled for 10 s to a temperature of about 700°C followed by controlled spray cooling (water+air mist) with a rate of about 27°C/s to an isothermal holding temperature of 400°C (Fig. 1a). The 3.3x170x1200 mm steel sheets were isothermally held at 400°C for 300 s in a furnace in order to enrich austenite in carbon. A final cooling step of sheets consisted of their air-cooling to room temperature. The steels containing 5% Mn were spray-cooled to 400°C immediately after finishing rolling (Fig. 1b).

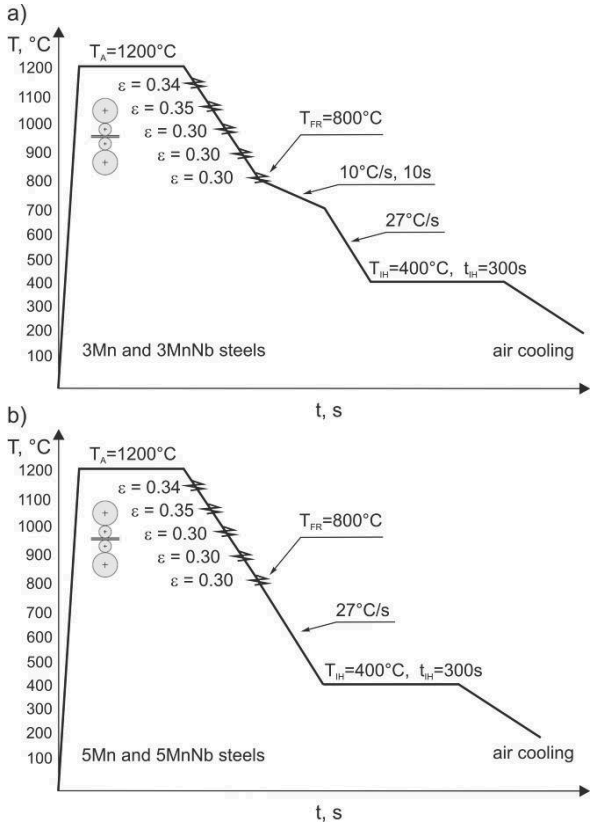

Fig. 1. Temperature-time-strain conditions of the thermo-mechanical rolling of 9 mm steel sheets to a thickness of 3.3 mm for 3Mn steels (a) and 5Mn steels (b); T_A - austenitizing temperature, T_{FR} - finishing rolling temperature, T_{IH} - isothermal holding temperature, t_{IH} - isothermal holding time

Metallographic specimens were taken along the rolling direction of the thermomechanically processed sheets. Evaluation of the degree of metallurgical cleanness of investigated steels with non-metallic inclusions was done on the basis of their fraction, type, size and morphology. Determination of stereological parameters of non-metallic inclusions was conducted using non-etched specimens with average area of 100 mm^2 (average values of 20 measured regions were calculated). For this purpose, LEICA Qwin automatic image analyzer cooperating with OPTON AXIOVERT 405M light microscope was used. The analysis was performed basing on the measurement of average size and the surface fraction of non-metallic inclusions as well as the ratio of their length to the thickness.

The analysis of the chemical composition of non-metallic inclusions and the effectiveness of their modification with rare earth elements was done with the use of JCXA 8230 X-ray microanalyser, implementing the accelerating voltage U=15 kV and the current I=30 nA. Qualitative point measurements of the chemical composition of particles were carried out using EDS whereas distribution maps of individual elements were registered using the WDS technique (better resolution than EDS). Micrographs were registered using secondary electrons (SEI) or back-scattered electrons (COMPO) at the magnification range between 2500-4000x.

3. Results and discussion

3.1. Quantitative analysis of non-metallic inclusions

Results of the quantitative analysis of non-metallic inclusions gathered in Table 2 as well as the micrographs in Figs. 2 and 3 clearly indicate the importance of the modification of non-metallic inclusions by rare earth elements. Mischmetal was not added to the 3Mn steel, what results directly in the higher sulphur concentration in this steel (Table 1) as well as the higher amount and surface fraction of non-metallic inclusions compared to three other steels (Table 2). The steels modified by rare earth elements (3MnNb, 5Mn, 5MnNb) contain about 0.005% S whereas the sulphur content in the 3Mn steel is three times higher. All the investigated steels are characterized by low concentration of phosphorus and gasses (Table 1). The low contents of N and O at the level of about 0.005 and 0.0004 ppm correspondingly are due to applied refining and vacuous process conditions.

The surface fraction of non-metallic inclusions for the 3Mn steel equals to 0.29%, what is about twice higher compared to three other steels modified by mischmetal (Table 2). The average number of inclusions per area is also the highest for the 3Mn steel. However, the average size of inclusions is similar for all the steels. It covers the range between 9 and 14 μm^2. The entire range of the inclusion area distribution is presented in Figs. 4a, 5a and 6a. It is clearly seen that the highest frequency have small non-metallic inclusions for all the steels investigated. The number of inclusions decreases with increasing their size. The non-metallic inclusions are very fine and possess the various morphology. The distribution of non-metallic inclusions at the longitudinal sections of the thermomechanically rolled sheets is shown in Figs. 2 and 3. The various fractions of globular, chain-like and elongated non-metallic inclusions can be seen.

Table 2.
Results of the quantitative analysis of non-metallic inclusions carried out by means of computer image analysis

Parameters of non-metallic inclusions	Minimum value				Maximum value				Average value				Standard deviation			
	3Mn	3MnNb	5Mn	5MnNb	3Mn	3MnNb	5Mn	5MnNb	3Mn	3MnNb	5Mn	5MnNb	3Mn	3MnNb	5Mn	5MnNb
Number of inclusions, [mm^{-2}]	203	97	95	101	347	208	191	202	279	142	129	145	78	64	55	67
Surface fraction, [%]	0.19	0.15	0.12	0.09	0.37	0.27	0.27	0.20	0.29	0.18	0.16	0.12	0.14	0.11	0.09	0.08
Surface area of inclusions, [μm^2]	0.57	0.45	0.41	0.37	39.7	49.3	34.7	34.2	10.7	13.5	13.2	8.9	6.4	7.6	7.7	4.1
Aspect ratio, l/t*	1.00	1.00	1.00	1.00	3.78	2.80	3.17	3.19	1.63	1.58	1.52	1.45	0.65	0.54	0.50	0.52

*l/t - the ratio of the length of the inclusion to its thickness

a) 3Mn steel

b) 3MnNb steel

Fig. 2. Distribution of non-metallic inclusions at the longitudinal sections of the thermomechanically rolled sheets; 3Mn steel is not modified by mischmetal (a) whereas 3MnNb steel is modified by mischmetal (b)

Fig. 3. Distribution of non-metallic inclusions at the longitudinal section of the thermomechanically rolled 5MnNb steel sheet; the steel is modified by mischmetal

The fractions of elongated inclusions are relatively small, especially for REE-modified steels (Figs. 2b and 3). The aspect ratios (the length of the inclusion to its thickness) of non-metallic inclusions have also relatively small values between 1.45 and 1.63 for all the steels (Table 2). It is obvious that the highest susceptibility to elongate in the rolling direction has the 3Mn steel. However, its aspect ratio (1.63) is just slightly higher than that of three other steels. The histograms in Figs. 4b, 5b and 6b show the distribution of the aspect ratio. The number of non-metallic inclusions with the aspect ratio higher than 2.2 is very small. The most elongated inclusions along the rolling direction occur for the steel non-modified by REE (Fig. 2a). The maximum values of the aspect ratio for this steel are equal to 3.8 (Table 2, Fig. 4b). Comparing the steels containing 3 and 5% Mn it should be concluded that the Mn content in a range of 3-5% does affect the parameters of non-metallic inclusions in a distinct way. The average values of the surface area of inclusions and aspect ratios (Table 2) as well as the distribution of these parameters (Figs. 4-6) are very similar. On the other hand, both the inclusion area and aspect ratio are smaller when compared to high-Mn steels [27].

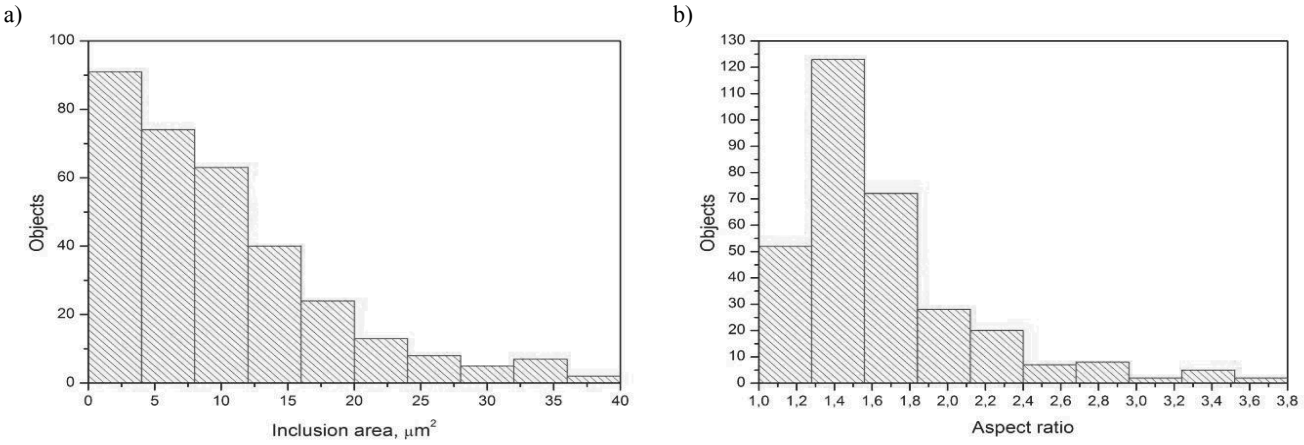

Fig. 4. Distribution of inclusion area (a) and aspect ratio (the ratio of the length of the inclusion to its thickness) at the longitudinal section of the thermomechanically rolled 3Mn steel sheet

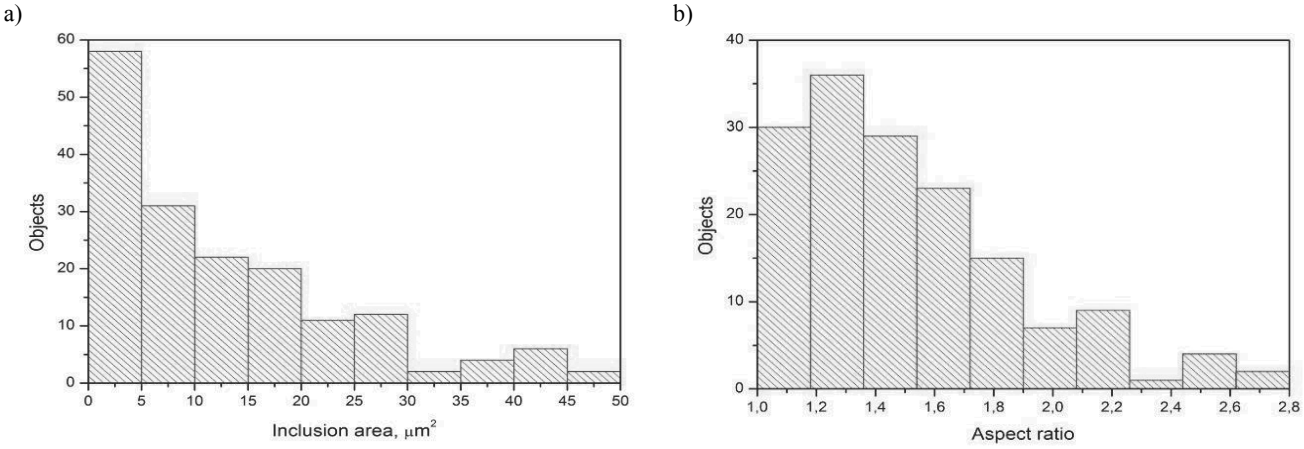

Fig. 5. Distribution of inclusion area (a) and aspect ratio (the ratio of the length of the inclusion to its thickness) at the longitudinal section of the thermomechanically rolled 3MnNb steel sheet

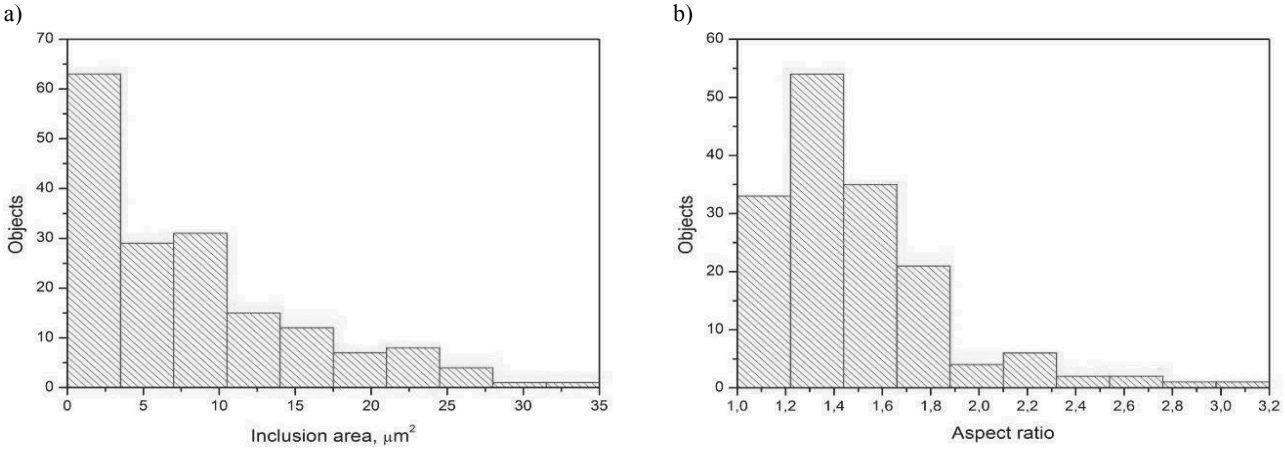

Fig. 6. Distribution of inclusion area (a) and aspect ratio (the ratio of the length of the inclusion to its thickness) at the longitudinal section of the thermomechanically rolled 5MnNb steel sheet

3.2. Qualitative analysis of non-metallic inclusions

Non-metallic inclusions present in the 3Mn steel containing the highest sulphur content are characterized by the strongest tendency to elongate along the rolling direction. Therefore, a few elongated inclusions can be seen in Fig. 7a. Moreover, the micrograph presents a globular inclusion with a diameter of about 5 μm. The spectrum of the central part of the large inclusion in Fig. 7b reveals that it is aluminium nitride. The number of nitrides is high because of the high chemical affinity of Al to N and its high content in the steel. Nitride inclusions are hard and difficult to deform during rolling.

a) 3Mn steel

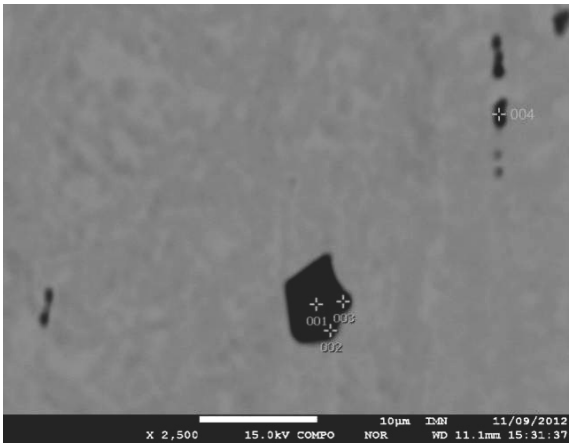

b) 001 point

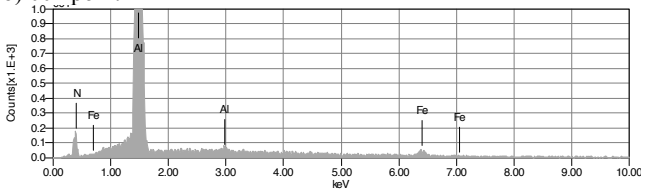

c) 002 point

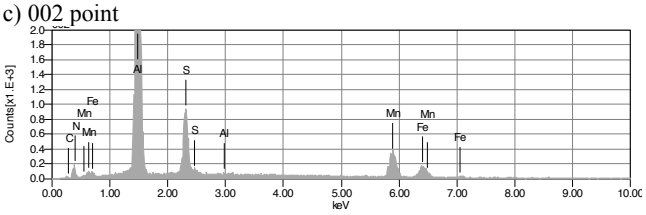

d) 004 point

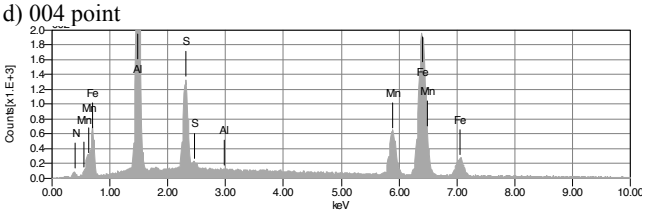

Fig. 7. The globular aluminium nitride and elongated complex sulfides; a - view of the inclusions, b - spectrum of the inclusion from the point 1, c - spectrum of the inclusion from the point 2, d - spectrum of the inclusion from the point 4 (3Mn steel)

The EDS analyses performed in the outer zones of the inclusion show that it is not a homogeneous particle. Manganese and sulphur were identified in these outside zones (Fig. 7c). The distribution maps of individual elements in Fig. 8 confirm the location of Mn and S at the outer bottom part of the analysed particle. It is interesting that the elongated smaller inclusions are also complex particles composed of AlN and MnS (Fig. 7d). Similar complex precipitates were also identified by Gigacher et al. [30] in the high-Mn steel containing 3% Al. It is obvious that the tendency of complex non-metallic inclusions to elongate along the rolling direction depends on the relative concentration of Mn, Al, S and N. It should be also noted that some concentration of oxygen is present at the outside zone of the large particle (Fig. 8). Al and N are uniformly distributed throughout the whole inclusion (Fig. 8).

a) 3MnNb steel

b)

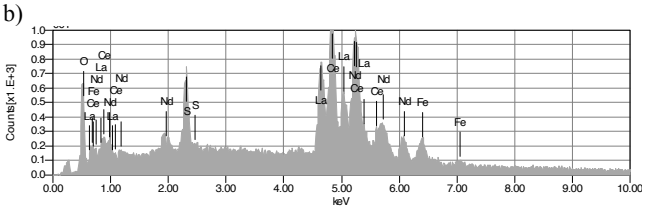

Fig. 9. The globular oxysulfide modified totally by Ce, La and Nb; a - view of the inclusion, b - spectrum of the inclusion from the point 1 (3MnNb steel)

The different chemical composition have non-metallic inclusions in the steels modified by REE. The result of the interaction between mischmetal and basic elements is obtaining complex oxysulfides with the low susceptibility to plastic deformation during hot-rolling. Figure 9 shows a typical, fine, globular-like particle at the longitudinal section of the thermomechanically rolled 3MnNb steel sheet. Spectrum lines (Fig. 9b) indicate the presence of Ce, La, Nd, Fe, O and S. The identification of Fe should be ascribed to the steel matrix due to a very small size of particles. There are no spectral lines from Al and Mn. It is concluded that the identified non-metallic inclusions of this type were modified totally by REE.

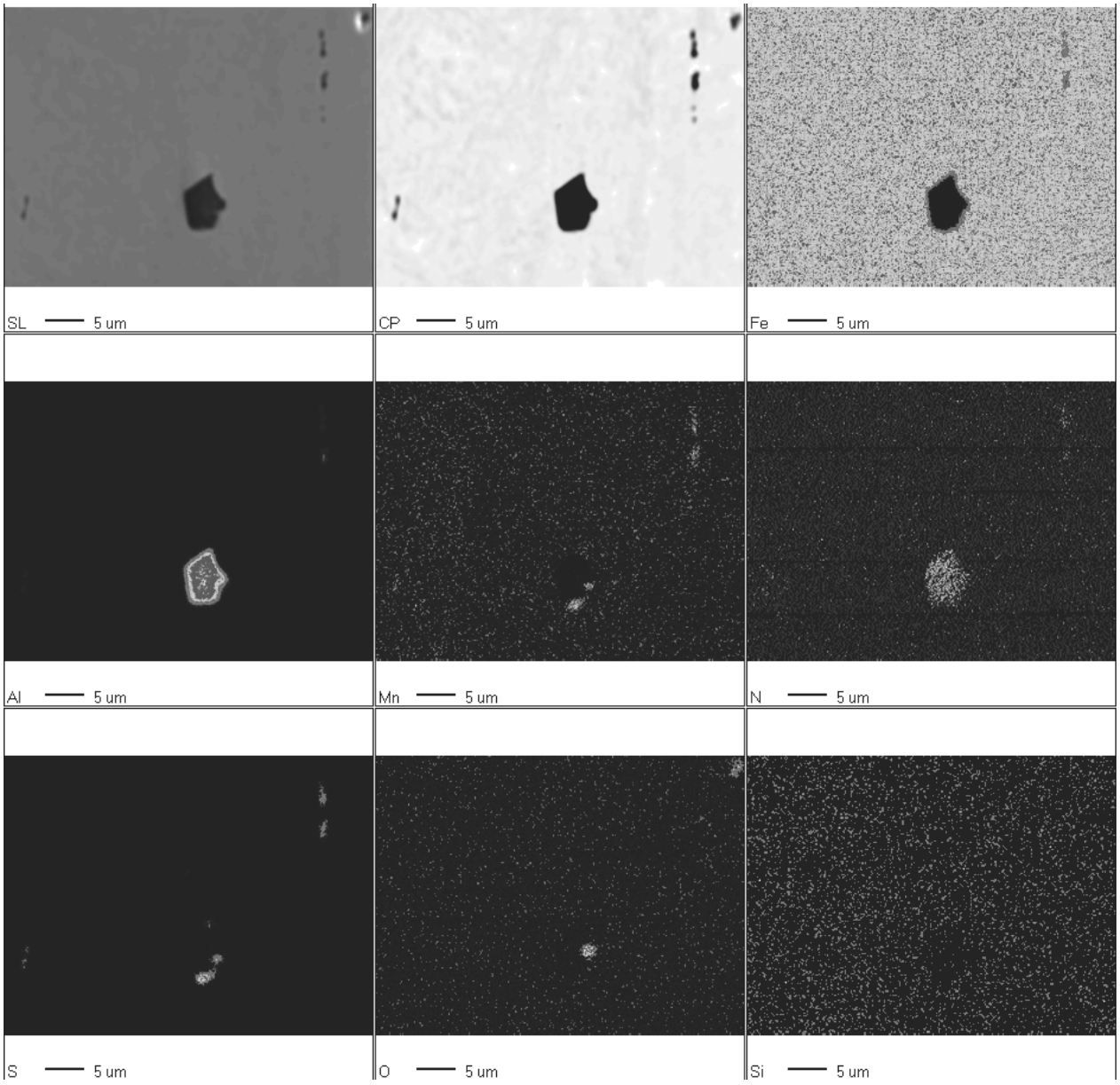

Fig. 8. Elemental mapping of aluminium nitride and complex, elongated sulfide inclusions located at the longitudinal section of the thermomechanically rolled 3Mn steel sheet

In agreement, the total modification of the chemical composition of non-metallic inclusions in the 3MnNb steel is confirmed by elemental mapping of the inclusion in Fig. 10. The micrograph shows clear that it is the oxysulfide containing only Ce, La and Nb. The rare earth elements and oxygen are distributed uniformly whereas sulphur is located at a core of the inclusion. Taking into account the high chemical affinity of REE to oxygen and sulphur and the high melting points of their compounds [27,34] they are presumably formed directly after their adding into the liquid bath. The melting points of oxides, sulfides or oxysulfides formed by REE are higher compared to the melting points of MnS (1539°C) and Al_2O_3 (2030°C). Hence, Ce, La and Nd displace Mn in sulfide inclusions and Al in oxide particles, forming phases of higher thermal stability and hardness.

The morphology and chemical composition of non-metallic inclusions of the steels containing 5% Mn are almost the same like in the 3MnNb modified by mischmetal. Moreover, the type of non-metallic inclusions is similar both for the Nb-bearing (Fig. 11) and Nb-free steel (Fig. 12). A large majority of particles, these are small, globular oxysulfides, oxides or more rarely sulfides of REE. Ce, La and Nd displaced Al and Mn totally forming non deformable particles (Fig. 11). The diameter of non-metallic inclusions containing REE covers a range between 1 and 5 μm.

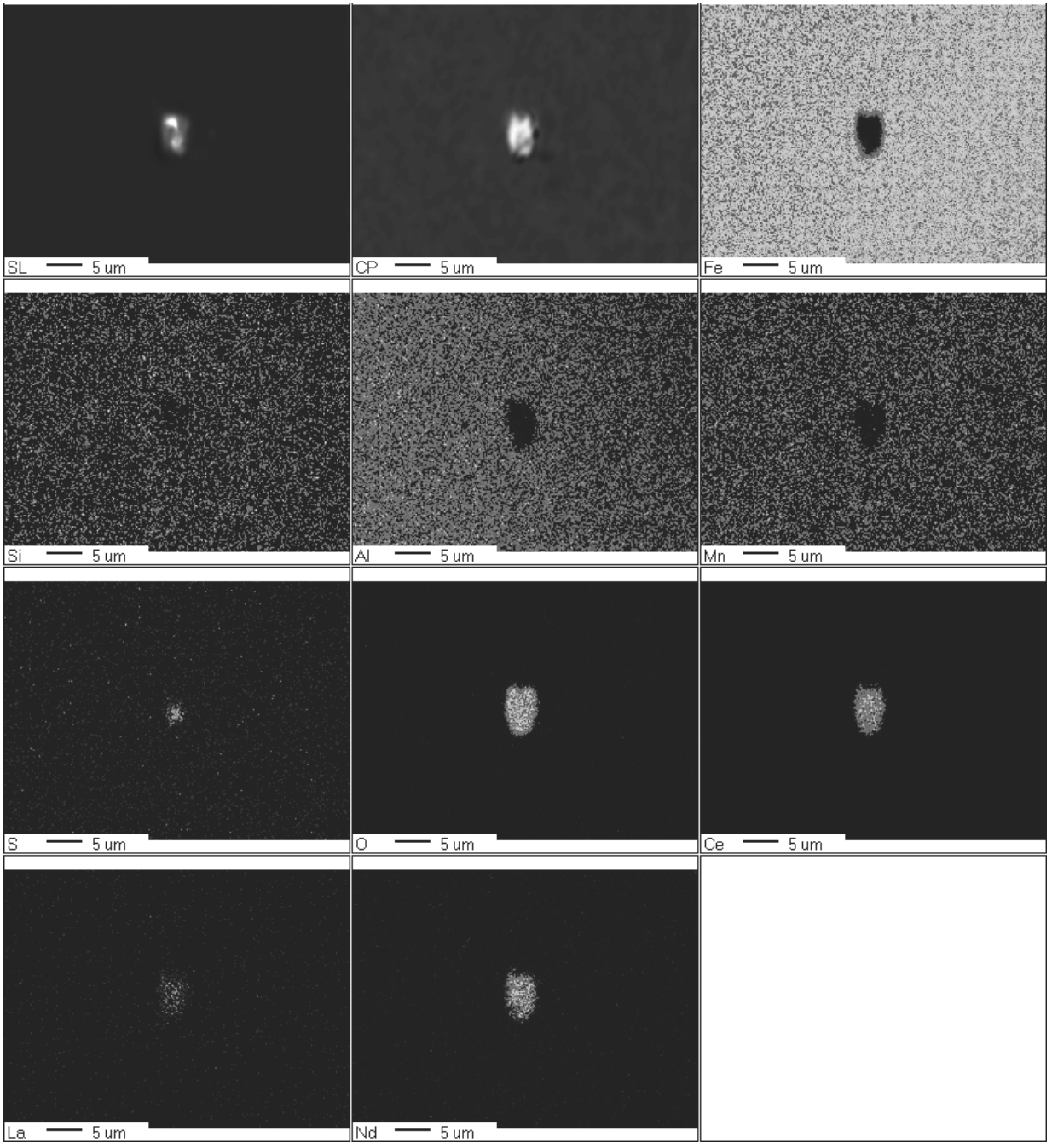

Fig. 10. Elemental mapping of the globular oxysulfide modified totally by Ce, La and Nb at the longitudinal section of the thermomechanically rolled 3MnNb steel sheet

It is interesting that small, slightly elongated aluminium nitrides were also sporadically observed in 5Mn steels (Fig. 11). It is not surprising in the 5Mn steel without Nb. However, taking into account the higher chemical affinity of Nb to N than Al to N the presence of AlN particles can be a little surprising in the Nb-bearing steel containing 5% Mn. On the other hand, any niobium carbonitrides were identified in the 5MnNb steel. It might be because of their high dispersion or dissolution of the total content of Nb microaddition in solid solution. The latter option is highly possible when the hampering effects of the high concentration of both Mn and Al on the precipitation of Nb(C,N) is considered [10,14]. This problem requires further TEM investigations and will be reported elsewhere.

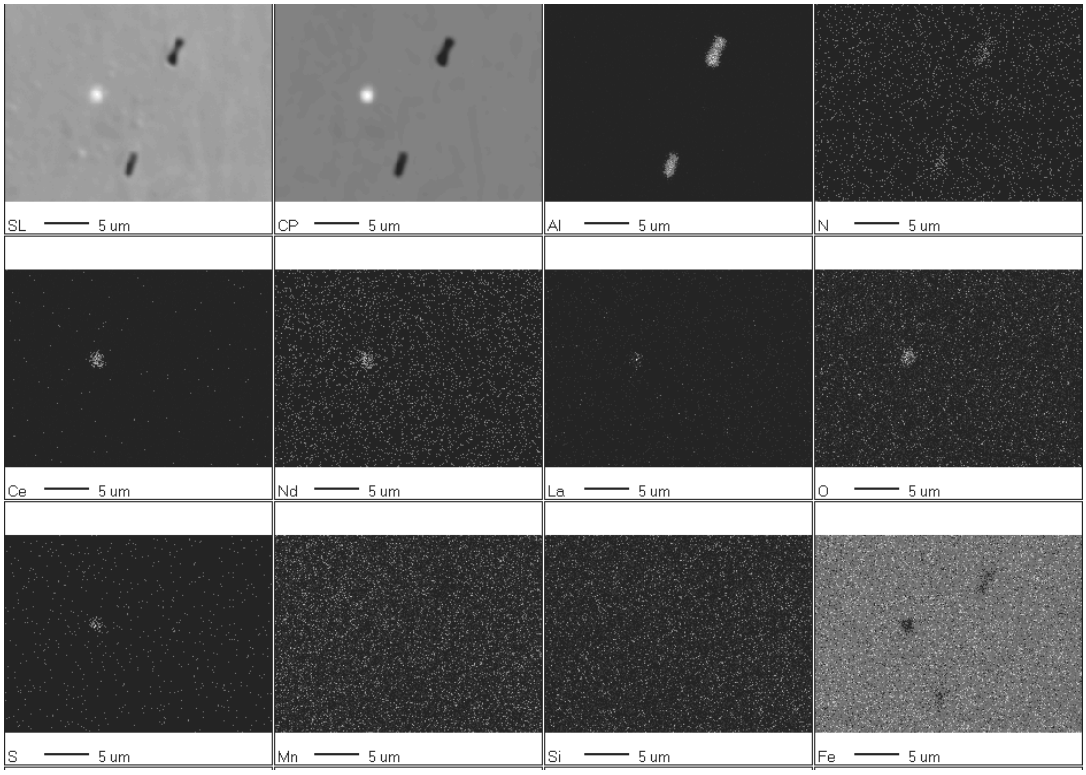

Fig. 11. Elemental mapping of different particles at the longitudinal section of the thermomechanically rolled 5MnNb steel sheet

a) 5Mn steel

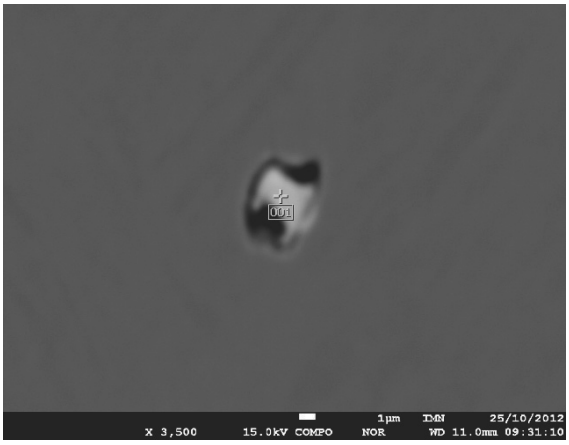

b)

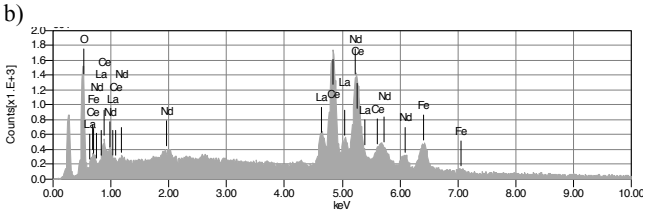

Fig. 12. The globular oxide modified totally by Ce, La and Nb; a - view of the inclusion, b - spectrum of the inclusion from the point 1 (5Mn steel)

4. Conclusions

The work included qualitative and quantitative investigations of the modification of non-metallic inclusions formed in thermo-mechanically rolled sheet steels with increased Mn and Al contents. It is concluded that the modification of liquid steels by rare earth elements affects positively the morphology and subsequent hot-working behaviour of these advanced high-strength steels. The first conclusion from the current study is that adding of mischmetal allows to obtain a low level of sulphur of about 0.005 wt.% whereas its content is three times higher in the 3Mn steel - not modified by REE. As a result, the surface fraction of non-metallic inclusions in the steels refined by mischmetal is in a range from 0.12 to 0.18% and twice larger for the 3Mn steel. On the other hand, the average surface area of particles - from 9 to 13 μm^2 - is almost the same for all the investigated steels. The inclusions are very fine and a part of them is slightly elongated along the rolling direction. However, the aspect ratio values are relatively small for the steels containing REE - from 1.45 to 1.58 - indicating the effectiveness of the modification of non-metallic inclusions. REE displaced Al and Mn forming globular, hardly-deformed oxysulfides, oxides and sulfides of REE. Small AlN particles were also sporadically revealed for the modified steels. Elongated pure manganese sulfides, complex MnS+AlN inclusions characterized by the lower tendency to deform in the rolling direction as well as globular AlN particles containing a mixture of MnS and Al_2O_3 at the outside zone of the inclusion were identified in the steel not subjected to the refining treatment.

Acknowledgements

The work was financially supported by the Polish Ministry of Science and Higher Education in a period of 2010-2012 in the framework of project No. N N508 590039.

References

[1] A. Pichler, S. Traint, T. Hebesberger, P. Stiaszny, E.A. Werner, Processing of thin multiphase steel grades, Steel Research International 78 (2007) 216-223.
[2] J. Adamczyk, A. Grajcar, Heat treatment and mechanical properties of low-carbon steel with dual-phase microstructure, Journal of Achievements in Materials and Manufacturing Engineering 22/1 (2007) 13-20.
[3] B. Gajda, A.K. Lis, A study of microstructure and phase transformations of CMnAlSi TRIP steel, Journal of Achievements in Materials and Manufacturing Engineering 31/2 (2008) 646-653.
[4] D. Krizan, B.C. De Cooman, Analysis of the strain-induced martensitic transformation of retained austenite in cold rolled micro-alloyed TRIP steel, Steel Research International 79/7 (2008) 513-522.
[5] A. Grajcar, Structural and mechanical behaviour of TRIP steel in hot-working conditions, Journal of Achievements in Materials and Manufacturing Engineering 30 (2008) 27-34.
[6] M. Mukherjee, S.B. Singh, O.N. Mohanty, Microstructural characterization of TRIP-aided steels, Materials Science and Engineering A 486 (2008) 32-37.
[7] O. Muransky, P. Hornak, P. Lukas, J. Zrnik, P. Sittner, Investigation of retained austenite stability in Mn-Si TRIP steel in tensile deformation condition, Journal of Achievements in Materials and Manufacturing Engineering 14 (2006) 26-30.
[8] A. Grajcar, Effect of hot-working in the $\gamma+\alpha$ range on a retained austenite fraction in TRIP-aided steel, Journal of Achievements in Materials and Manufacturing Engineering 22/2 (2007) 79-82.
[9] H. Yu, S. Li, Y. Gao, Deformation behavior of the constituent phases for cold-rolled TRIP-assisted steels during uniaxial tension, Materials Characterization 57 (2006) 160-165.
[10] A. Grajcar, R. Kuziak, Softening kinetics in Nb-microalloyed TRIP steels with increased Mn content, Advanced Materials Research 314-316 (2011) 119-122.
[11] P.J. Gibbs, E. De Moor, M.J. Merwin, B. Clausen, J.G. Speer, D.K. Matlock, Austenite stability effects on tensile behaviour of manganese-enriched-austenite transformation-induced plasticity steel, Metallurgical and Materials Transactions A 42A (2011) 3691-3702.
[12] A. Grajcar, E. Kalinowska-Ozgowicz, M. Opiela, B. Grzegorczyk, K. Gołombek, Effects of Mn and Nb on the macro- and microsegregation in high-Mn high-Al content TRIP steels, Archives of Materials Science and Engineering 49/1 (2011) 5-14.
[13] G.A. Thomas, J.G. Speer, D.K. Matlock, Quenched and partitioned microstructures produced via Gleeble simulations of hot-strip mill cooling practices, Metallurgical and Materials Transactions A 42A (2011) 3652-3659.
[14] A. Grajcar, R. Kuziak, Effects of Nb microaddition and thermomechanical treatment conditions on hot deformation behaviour and microstructure of Mn-Al TRIP steels, Advanced Science Letters 15 (2012) 332-336.
[15] P.S. Bandyopadhyay, S.K. Ghosh, S. Kundu, S. Chatterjee, Evolution of microstructure and mechanical properties of thermomechanically processed ultrahigh-strength steel, Metallurgical and Materials Transactions A 42A (2011) 2742-2752.
[16] A. Grajcar, Determination of the stability of retained austenite in TRIP-aided bainitic steel, Journal of Achievements in Materials and Manufacturing Engineering 20/1-2 (2007) 111-114.
[17] K. Sugimoto, K. Nakano, S.M. Song, T. Kashima, Retained austenite characteristics and stretch-flangeability of high-strength low-alloy TRIP type bainitic sheet steels, ISIJ International 42/4 (2002) 450-455.
[18] J. Adamczyk, A. Grajcar, Heat treatment of TRIP-aided bainitic steel, International Journal of Microstructure and Materials Properties 2 (2007) 112-123.
[19] A.K. Lis, J. Lis, L. Jeziorski, Advanced ultra-low carbon bainitic steels with high toughness, Journal of Materials Processing Technology 64 (1997) 255-266.
[20] A. Grajcar, R. Kuziak, W. Zalecki, Third generation of AHSS with increased fraction of retained austenite for the automotive industry, Archives of Civil and Mechanical Engineering 12 (2012) 334-341.
[21] L.A. Dobrzański, A. Grajcar, W. Borek, Microstructure evolution of high-manganese steel during the thermomechanical processing, Archives of Materials Science and Engineering 37/2 (2009) 69-76.
[22] A. Grajcar, S. Kołodziej, W. Krukiewicz, Corrosion resistance of high-manganese austenitic steels, Archives of Materials Science and Engineering 41/2 (2010) 77-84.
[23] T. Bator, Z. Muskalski, S. Wiewiórowska, J.W. Pilarczyk, Influence of the heat treatment on the mechanical properties and structure of TWIP steel in wires, Archives of Materials Science and Engineering 28/6 (2007) 337-340.
[24] L.A. Dobrzański, W. Borek, Hot deformation and recrystallization of advanced high-manganese austenitic TWIP steels, Journal of Achievements in Materials and Manufacturing Engineering 46/1 (2011) 71-78.
[25] L.A. Dobrzański, W. Borek, M. Ondrula, Thermo-mechanical processing and microstructure evolution of high-manganese austenitic TRIP-type steels, Journal of Achievements in Materials and Manufacturing Engineering 53/2 (2012) 59-66.
[26] E. De Moor, D.K. Matlock, J.G. Speer, M.J. Merwin, Austenite stabilization through manganese enrichment, Scripta Materialia 64 (2011) 185-188.
[27] A. Grajcar, U. Galisz, L. Bulkowski, Non-metallic inclusions in high manganese austenitic alloys, Archives of Materials Science and Engineering 50/1 (2011) 21-30.
[28] G. Lacroix, T. Pardoen, P.J. Jacques, The fracture toughness of TRIP-assisted multiphase steels, Acta Materialia 56/15 (2008) 3900-3913.

[29] P. Kaushik, H. Yin, Thermodynamics, engineering and characterization of inclusions in advanced high-strength steels, Iron and Steel Technology 9/12 (2012) 165-185.
[30] G. Gigacher, W. Krieger, P.R. Scheller, C. Thomser, Non-metallic inclusions in high-manganese-alloy steels, Steel Research International 76/9 (2005) 644-649.
[31] S. Yang, L. Zhang, L. Sun, J. Li, K.D. Peaslee, Investigation on $MgO{\cdot}Al_2O_3$-based inclusions in steels, Iron and Steel Technology 9/8 (2012) 245-258.
[32] M. Opiela, M. Kamińska, Influence of the rare-earth elements on the morphology of non-metallic inclusions in microalloyed steels, Journal of Achievements in Materials and Manufacturing Engineering 47/2 (2011) 149-156.
[33] C. Luo, U. Stahlberg, Deformation of inclusions during hot rolling of steels, Journal of Materials Processing Technology 114 (2001) 87-97.
[34] K. Bolanowski, Influence of rare-earth elements on the structure and properties of steel, Metallurgical News 7-8 (2004) 323-325 (in Polish).
[35] M. Opiela, A. Grajcar, Modification of non-metallic inclusions by rare-earth elements in microalloyed steels, Archives of Foundry Engineering 12/2 (2012) 129-134.